Mechatronics xxx (2013) xxx–xxx

Contents lists available at ScienceDirect

Mechatronics

journal homepage: www.elsevier.com/locate/mechatronics

Self-tuning fault diagnosis of MEMS

Afshin Izadian *

Energy Systems and Power Electronics Laboratory, The Purdue School of Engineering and Technology, IUPUI, Indianapolis, IN 46202, USA

ARTICLE INFO

Article history:
Received 7 April 2013
Accepted 26 August 2013
Available online xxxx

Keywords:
MEMS
Fault diagnosis
Self-tuning

ABSTRACT

Multiple-model adaptive estimation techniques have been previously successfully applied to fault diagnosis of microsystems. Their diagnosis performance highly depends on the accuracy of modeling techniques used in representing faults. This paper presents the application of a self-tuning forgetting factor technique in the modeling of faults in MEMS and its effects on diagnosis performance compared with the application of Kalman filters and fixed gain estimation techniques. The self-tuning-based modeling used in the diagnosis algorithm was experimentally implemented. It demonstrated superior results compared to Kalman filter and fixed gain estimation techniques by accelerating the diagnosis process.

1. Introduction

Fault in MEMS can be originated from local defects, parameter tolerances, design problems, operation, and/or system level defects [1]. For instance, a fault might happen because of a fracture in different parts of the device such as suspension springs or fingers. In open-to-air applications, there is a chance that dust and other particles could fall on the structure of the device, which may cause a sudden mass change. In addition, the silicon-made structures absorb humidity from the air, which results in changes in the mechanical properties of the suspension springs. For devices operating in vacuum conditions, any damage to the container might result in a loss of vacuum and consequently change the viscosity. In any of these cases, asymmetries affect the behavioral changes and unwanted deviations from the desired output, which can be modeled with mathematical expressions [2–10,15,26–28].

Performance in model-based fault diagnosis of MEMS [25] requires accurate representations of the faults. The model of the system should represent the dynamics of the observable systems and generate residual signals of systems under various conditions. However, in noise-contaminated environments Kalman filters may be required to prevent performance deterioration [11–13]. Other techniques may require proper forgetting-factor techniques to identify accurate and effective models. In our previous work, we used Kalman filters to overcome the effect of measurement and system noise [4,12], and the utilization of fixed forgetting factor to improve the diagnosis performance [4,11].

Slowly varying parameter systems requires system identification techniques to accurately measure the expected output signals, leading to a high-performance diagnosis [11]. The modeling process using Kalman filters or estimation-based techniques requires accurate system and measurement noise evaluations or several trials and errors to tune the fixed forgetting factors. Accurate noise evaluation is required in Kalman filters. Noise under- and over-estimation resulted in a low performance residual generation and evaluation process, thus lowering the sensitivity of the fault diagnosis [11–14]. The estimation-based techniques require a manual adjustment of the estimator gains for better results. A history of the variation needs to be selected in the parameter estimation blocks. However, the accuracy highly depends on the forgetting factor gain obtained in a trial and error. The gain has to be re-tuned if the system parameters shift over time or if the noise level changes.

In this paper, a self-tuning-based parameter estimation technique is used to identify the system parameters and generate precise residual signals. The performance of fault diagnosis depends on the accuracy of the self-tuning-based estimation technique. The algorithm is implemented in hardware-in-loop through fast prototyping devices and the diagnosis performance is compared with those obtained from Kalman and fixed gain forgetting factor estimation approaches.

2. MEMS LCRs and fault models

The complicated structure of MEMS devices, like gyroscopes and micro-mirrors, can be simplified into several basic elements such as parallel plate actuators and lateral comb resonators (LCRs). MEMS LCRs consist of two sets of fixed combs on both sides of a moving stage. The shuttle (moving part) has a comb-shaped structure with fingers placed in the spaces between those on the fixed structure (Fig. 1). The shuttle is suspended on two sets of springs and can be laterally displaced by the electrostatic force generated

* Tel.: +1 317 274 7881.
E-mail address: aizadian@iupui.edu

0957-4158/$ - see front matter © 2013 Elsevier Ltd. All rights reserved.
http://dx.doi.org/10.1016/j.mechatronics.2013.08.006

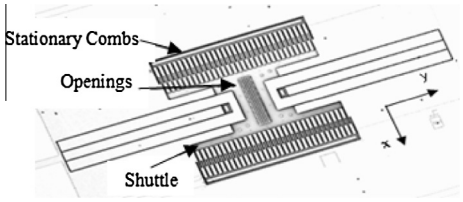

Fig. 1. MEMS lateral comb resonator.

between the comb fingers. This system can be modeled as a second-order mass-spring-damper dynamic.

LCRs have been modeled as a second-order mass-spring-damper system [3–5]. Loss of vacuum, severe shocks and manufacturing defects are common types of faults in microsystems, which are modeled by damping coefficient, mass, and spring constant variations. Severe structural damages might also impair the device and cause failure. In fault diagnosis and supervisory monitoring of MEMS, some specific parameter variations might be of particular interest and create signature faults. Structural variations can also be modeled as a shift in the values of these parameters.

A second-order system, MEMS displacement, can be expressed by

$$F_e = m\ddot{q} + \beta\dot{q} + 2k_s q + F_d, \tag{1}$$

where q is the displacement, m is the mass of the center comb (shuttle), K_s is half of the spring constant, β is the damping coefficient, and F_d is the force due to the load and F_e is the electrostatic force of the actuator. Fig. 2 shows the schematic diagram of the MEMS LCR dynamical system. Fig. 2 shows the difference of F_e and F_d as F.

The frequency response of an ideal (design) second-order governing Eq. (1) and the actual measurement of the phase and amplitude from a fabricated MEMS LCR are shown in Fig. 3. The shift in resonant frequency resulted from the manufacturing imperfections.

State space model of the second-order system can be represented by

$$\begin{cases} \dot{x} = Ax + Bu \\ y = Cx \end{cases}, \tag{2}$$

where $A = \begin{bmatrix} 0 & 1 \\ \frac{-2k_s}{m} & \frac{-\beta}{m} \end{bmatrix}, B = \begin{bmatrix} 0 \\ \frac{1}{m} \end{bmatrix}$, and $C = [1 \quad 0]$ are the system, input, and output matrices respectively, and $x=[x_1\ x_2]^T$ is the state variable vector, and y is the output of the system. Considering the C matrix elements, one can obtain $y = x_1$.

Several distinct models of fault can be obtained by considering different values of m, k_s, and β. A set of these models $\{f_k \in \Delta | f_k = f(m_k, \beta_k, k_{sk}, F_{ek}, F_{dk}), k = 1, 2, \ldots, n\}$ can be selected from the fault domain Δ such that it includes all the desired fault models. The parameters of the kth fault-representing model are m_k, β_k, k_{sk}, F_{ek}, F_{dk}. The model can be rewritten as

$$f_k : \begin{cases} x_k(t_i) = \Phi_k x_k(t_{i-1}) + \Gamma_k u(t_{i-1}) + G_k w_k(t_i) \\ z_k(t_i) = H_k x_k(t_i) + v_k(t_i) \end{cases}, \tag{3}$$

where x_k is the kth-system state space variable, $\Phi_k = e^{AT}$ is the discrete system matrix, $\Gamma_k = \left(\int_0^T e^{A\tau} d\tau\right) B, H_k = C$ is the discrete input matrix, u is the input vector, G_k is the model's input noise matrix, w_k is the input noise with zero mean and variance of

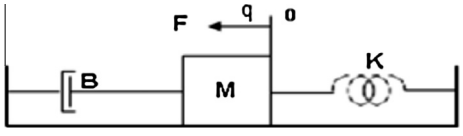

Fig. 2. Mass-spring-damper, schematic model of lateral comb resonator.

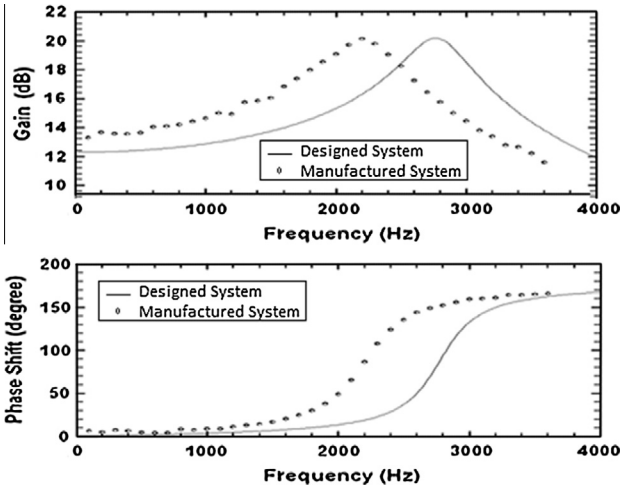

Fig. 3. The frequency response (Bode-plot) of the simulated designed system and the measured values from a fabricated MEMS LCR [17].

$$E\{w_k(t_i)w_k^T(t_j)\} = \begin{cases} Q_k, t_i = t_j \\ 0, t_i \neq t_j \end{cases}, \tag{4}$$

Z_k is the measurement vector, H_k is the output matrix, and $v_k(t_i)$ is the output of measurement noise, independent from w_k, with a zero mean value as

$$E\{v_k(t_i)v_k^T(t_j)\} = \begin{cases} R_k, t_i = t_j \\ 0, t_i \neq t_j \end{cases}. \tag{5}$$

To obtain the residual signal of each model, the output signal of that model can be obtained and subtracted from the output of the MEMS device as

$$r_k(t_i) = y(t_i) - H_k x_k(t_i)). \tag{6}$$

3. Self-tuning estimation

To obtain models of fault, the history of the parameter variation can be utilized through a recursive least square method with the forgetting factor. The forgetting factor considers the effects of the previous samples on the performance of the estimation. The diagnosis performance significantly changes as the forgetting factor is adjusted. Consider an auto regressive moving average (ARMA) system representing the kth subsystem obtained from system (3) at a time instant using $\frac{z_k(t_i)}{u_k(t_i)} = H_k(zI - \Phi_k)^{-1}\Gamma_k$, which can also be expressed as

$$f_k : z_k(t_{i+1}) = b_0 u(t_i) + \cdots + b_m u(t_{i-m}) - a_1 z_k(t_i) - \cdots - a_n z_k(t_{i-n+1}), \tag{7}$$

where a_i is the coefficient of the denominator polynomial (input polynomial), b_i is the coefficient of the numerator (output polynomial) of the system, and u and z_k are the input and output signals of the kth subsystem. The unknown parameter values of the system are listed in a vector as $\theta^T = [b_0, b_1, \ldots, b_m, a_1, a_2, \ldots, a_n]$.

The size of the unknown vector is $l = m + n + 1$ where $m + 1$ represents the order of the numerator and denominator polynomials respectively. The model's input–output data sets can be expressed in a regressor matrix as

$$h^T(t_i) = [u(t_i), u(t_{i-1}), \cdots, u(t_{i-m}), -z_k(t_i) - z_k(t_{i-1}), \cdots, -z_k(t_{i-n+1})]. \tag{8}$$

The subsystem can be represented in compact form as $z_k(t_{i+1}) = h^T(t_i)\theta(t_i)$. The estimated output can be obtained by substituting an estimate of parameter values $\hat{\theta}(t_i)$ in (9) as $\hat{z}_k(t_{i+1}) = h^T(t_i)\hat{\theta}(t_i)$. The parameters of the system were extracted recursively utilizing the RLS estimation algorithm as [18,19]

Please cite this article in press as: Izadian A. Self-tuning fault diagnosis of MEMS. Mechatronics (2013), http://dx.doi.org/10.1016/j.mechatronics.2013.08.006

$$\hat{\theta}(t_{i+1}) = \hat{\theta}(t_i) + \eta(t_i)h(t_i)\{1 + h^T(t_i)\eta(t_i)h(t_i)\}^{-1}\{z(t_{i+1}) - h^T(t_i)\hat{\theta}(t_i)\}, \quad (9)$$

where $\eta(t)$ is the covariance matrix. This matrix is defined and updated by

$$\eta(t_{i+1}) = \eta(t_i) - \{1 + h^T(t_i)\eta(t_i)h(t_i)\}^{-1}\{\eta(t_i)h(t_i)h^T(t_i)\eta(t_i)\}. \quad (10)$$

Applying the forgetting factor RLS (FFRLS), the time-varying parameters were estimated by introducing the forgetting factor λ as follows [18,19]

$$\hat{\theta}(t_{i+1}) = \hat{\theta}(t_i) + \eta(t_i)h(t_i)\{\lambda + h^T(t_i)\eta(t_i)h(t_i)\}^{-1}\{z(t_{i+1}) - h^T(t_i)\hat{\theta}(t_i)\}. \quad (11)$$

The covariance matrix, $\eta(t)$ can be re-written as

$$\eta(t_{i+1}) = \frac{1}{\lambda}\left[\eta(t_i) - \{\lambda + h^T(t_i)\eta(t_i)h(t_i)\}^{-1}\{\eta(t_i)h(t_i)h^T(t_i)\eta(t_i)\}\right], \quad (12)$$

where λ, the self-tuned forgetting factor, can be derived according to the following procedure. For optimum forgetting factor adjustment, the normalized variance with respect to σ_ω^2 can be re-written as

$$R_i = 1 + H_i P'_{i-1} H_i^T. \quad (13)$$

In practical implementations, an unbiased estimation of R_i can be obtained from the measurement data [21] as

$$\widehat{R}_i = \frac{1}{\sigma_\omega^2}\frac{1}{i-1}\sum_{k=1}^{i} w_k w_k^*, \quad i = 1, 2, \ldots. \quad (14)$$

The estimated value can be calculated recursively as

$$\widehat{R}_i = \frac{1}{\sigma_\omega^2}\frac{\lambda_{i-1}\widehat{R}_{i-1} + w_k w_k^*}{\gamma_i}, \quad (15)$$

where

$$\gamma_i = 1 + \lambda_{i-1}\gamma_{i-1}. \quad (16)$$

The initial conditions might start at $\lambda_0 = 1, \widehat{R}_0 = 0,$ and $\gamma_0 = 0$. The value of λ_i, due to the noise in the system, might be larger than 1. There is almost no model that can ensure that the forgetting factor value under all conditions remains limited within $\lambda_i \in (0, 1]$ [21]. Therefore, in practical implementation, there is a necessity to consider a reasonable limit on λ_i. In this regard, consider the initial value of λ_i as

$$\lambda_i = \frac{\lambda_{i-1}(1 + H_i P'_{i-1} H_i^T)}{\widehat{R}_i}, \quad (17)$$

where $P'_i = \frac{P_i}{\lambda_i}$. To limit the forgetting factor to $\lambda_i \in (0, 1]$, a mapping procedure [20] should be considered as

$$\lambda_i = \lambda_{i-1} + \mu \cdot \mathrm{sgn}(\lambda_i - \lambda_{i-1}), \quad (18)$$

where μ is the step size determined according to the parameter variation rate and the noise, and P is the covariance matrix and is updated using $P(n+1) = G_k Q G_k^T + \Phi_k P(n)\Phi_k^T - \Phi_k P(n) H_k [R + H_k P(n) H_k^T]^{-1} H_k P(n)\Phi_k^T$. For real-time implementation of the self-tuning forgetting factor, there is no need to estimate σ_ω^2 [13,21]. It can be proven that the forgetting factor can be mapped to the region of $\lambda_i \in (0, 1]$ as follows:

If $\lambda_{i-1} \geqslant 1$, there exists a μ such that $0 < \lambda_{i-1} + \mu \leqslant 1$. This yields $0 < \lambda_i \leqslant 1$, which imposes the existence of a negative μ. As $\lambda_{i-1} \geqslant 1$ and $0 < \lambda_i \leqslant 1$, this yields $\mathrm{sgn}(\lambda_i - \lambda_{i-1}) \leqslant 0$. Therefore, $\lambda_i = \lambda_{i-1} + \mu\mathrm{sgn}(\lambda_i - \lambda_{i-1})$ guarantees the existence of a bounded forgetting factor and $\lambda_i \in (0, 1]$.

If $0 < \lambda_{i-1} \leqslant 1$, there exists a μ such that $0 < \lambda_{i-1} + \mu \leqslant 1$. This yields $0 < \lambda_i \leqslant 1$, which imposes the existence of a positive μ. As $0 < \lambda_{i-1} \leqslant 1$ and $0 < \lambda_i \leqslant 1$, this yields $\mathrm{sgn}(\lambda_i - \lambda_{i-1}) > 0$. Therefore, $\lambda_i = \lambda_{i-1} + \mu\mathrm{sgn}(\lambda_i - \lambda_{i-1})$ guarantees the existence of a bounded forgetting factor and $\lambda_i \in (0, 1]$.

In MEMS fault diagnosis, the initial forgetting factor value and variance were considered as $\lambda_0 = 1, \widehat{R}_0 = 0$, with a step size of $\mu = 0.0001$.

4. Design of experiments

The model-based fault diagnosis structure is shown in Fig. 4. Several models $f_1 - f_n$ can be designed to accurately represent n signature faults for the diagnosis of any system. f_i is the ith fault-representing model, which can contain unique parameter variations from the original system that result in the output deviation from the desired operation. In a residual generation unit, all models are excited with the same input that drives the actual system. Each fault-representing model generates a different output, which, at a time instant, should not match with any of the other outputs. If there is a fault in the system, the actual system's output will match with the output of one of the fault representing models. Therefore, the difference between their outputs, the residual signal, becomes a zero mean value. The existence of noise in the actual settings results in the loss of fault information (small signal-to-noise ratio). Hence, the fault diagnosis becomes indifferent for small parameter variations, resulting in a low-sensitivity diagnosis. Several modeling techniques have been introduced to estimate the output of the fault models in a noisy environment. In this section, residual generation techniques, such as Kalman filters [12,22] and output estimation units are used in residual signal generation. Residual signals are used in an evaluation center to determine the mean value, covariance, and probabilities, based on the history of variation.

To create the faults and to demonstrate the effectiveness of self-tuning forgetting factor-based fault diagnosis, two identical structures of MEMS LCRs with different parameters were designed and manufactured. The parameters of the two MEMS devices are listed in Table 1. The fault was created by recording the displacement of the two devices (excited individually) and joining them together to obtain a fault stimulating waveform. The point of fault was created

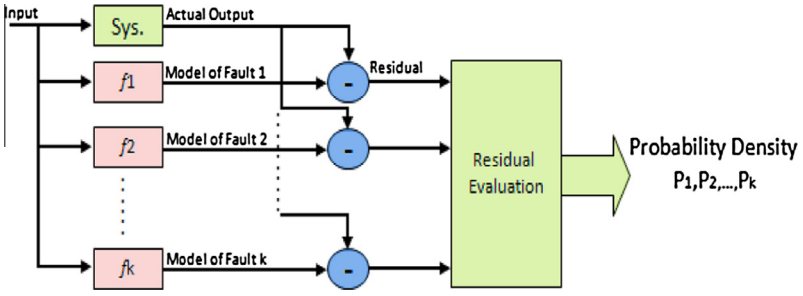

Fig. 4. Multiple-model residual generation and residual evaluation.

Please cite this article in press as: Izadian A. Self-tuning fault diagnosis of MEMS. Mechatronics (2013), http://dx.doi.org/10.1016/j.mechatronics.2013.08.006

Table 1
Estimated Parameters of Two Fabricated Systems.

	Mass (kg)	K_s (Nm^{-1})	Beta (Nm^{-1} s)
Device 1	2.3856e−10	0.0193	7.563e−7
Device 2	2.2429e−10	0.0448	1.385e−6

at a zero crossing displacement to emulate a hard-to-diagnose operating point for the diagnosis algorithm evaluation. A Polytech® optical Doppler laser vibrometer was used to measure the displacement of the MEMS LCRs. The data was recorded using dSPACE type DS1103.

The unified displacement waveform resulting from device 1 and device 2 while excited by a $10\sin(4000\pi t)$ volt signal is shown in Fig. 5. The fault occurred at point 1 at the 1886th data sample. Point 2 on this figure indicates the first displacement peak after the fault. The point of fault was created at zero displacement to emulate an extremely difficult operating point for the fault diagnosis algorithm. If the fault occurred at the peak of the displacement, a sudden change would have generated stronger variations and a higher signal-to-noise ratio (SNR), and the algorithm would be able to diagnose it rapidly. In practical implementation, each MEMS device is monitored individually and has separate signature fault models. The resulting waveform was used in verifying the algorithm and evaluating the fault diagnosis performance [23].

The self-tuning forgetting factor fault diagnosis algorithm was implemented in Matlab. The recorded data was used to verify the diagnosis performance.

5. Fault diagnosis

In the multiple model adaptive estimation (MMAE) technique, as shown in Fig. 4, several models run in parallel while excited with input similar to that of the actual system. The difference between the output signals of the individual models and those of the actual system is that those of the actual system generate residual signals. To evaluate and extract the fault information from the residual signals, an evaluation algorithm should continuously monitor the residual signal variations. If the output of any model matches the output of the actual system and makes the mean value of the residual signal zero, then the covariance of that signal can be computed [11,12,14] by

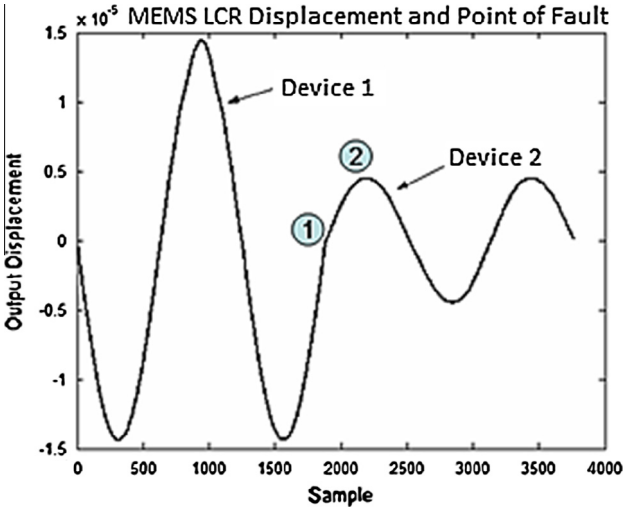

Fig. 5. Displacement of LCR and the point of fault. Point 1 determines the location of the fault, and point 2 determines the first peak of the second system output.

$$\psi_k = H_k P_k H_k^T. \tag{19}$$

In this work, probability-based residual signal evaluation was applied to the residual signals generated from the techniques described in Section 3. Conditional probability density functions of the kth model considering the history of measurement $Z(t_{i-1}) = [z^T(t_1)\ldots z^T(t_{i-1})]$ are expressed [16,22] as

$$f_{z(t_i)|h,z(t_{i-1})}(z_i|h_k, Z_{i-1}) = \beta_k \exp\{\cdot\}, \tag{20}$$

with

$$\beta_k = \frac{1}{(2\pi)^{l/2}|\psi_k|^{l/2}}, \tag{21}$$

and

$$\{\cdot\} = \left\{-\frac{1}{2} r_k^T(t_i)\psi_k^{-1} r_k(t_i)\right\}, \tag{22}$$

where r_k is the residual signal as defined in (7). The conditional probability density functions require *a priori* samples to compute the current values and should be normalized over a complete sum of the conditional probabilities of all the systems [22]. The largest conditional probability among all can be used as an indicator of fault in the systems (note that each fault-representing system should be modeled separately). In addition, they can associate weight to the outputs of the systems to define the weighted output for each fault-model. In some applications, where probabilities change rapidly and make the output of the system unpredictable, the output should then be compared with a threshold [16,24]. The conditional probability evaluation of the k^{th} system is defined as

$$p_k(t_i) = P\{h = h_k | Z(t_i) = Z_i\}. \tag{23}$$

This value can also be computed [22] by

$$P_k(t_i) = \frac{f_{z(t_i)|h,z(t_{i-1})}(z_i|h_k, Z_{i-1}) \cdot p_k(t_{i-1})}{\sum_{j=1}^{k} f_{z(t_i)|h,z(t_{i-1})}(z_i|h_j, Z_{i-1}) \cdot p_j(t_{i-1})}. \tag{24}$$

To demonstrate the advantages of using self-tuning forgetting factor in fault diagnosis, the Kalman filter and the fixed forgetting factor were also implemented, and their fault diagnosis profile was recorded for the same set of fault data. Interested readers are referred to our previous research for Kalman and fixed forgetting factor techniques [4,11,12].

Fig. 6 illustrates the forgetting factor generation during the fault diagnosis. As the figure shows, the forgetting factor value was automatically adjusted to the set of $\lambda_i \in (0, 1]$. Accordingly, the residual signals are shown in Fig. 7. Fig. 8 shows the probability generation and diagnosis performance resulting from using the Kalman filter, the fixed forgetting factor, and the self-tuning forgetting factor methods.

Fig. 7 illustrates the effects of the similar behavior of one model and the actual MEMS. As any model matches the MEMS device, its

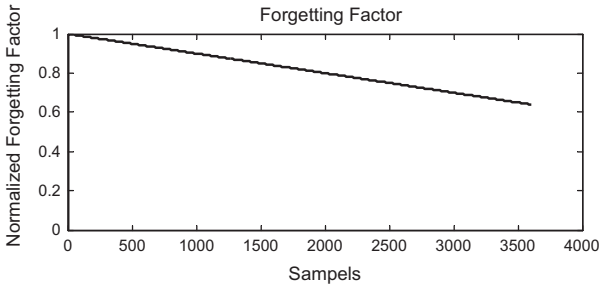

Fig. 6. Forgetting factor variation during fault diagnosis.

Please cite this article in press as: Izadian A. Self-tuning fault diagnosis of MEMS. Mechatronics (2013), http://dx.doi.org/10.1016/j.mechatronics.2013.08.006

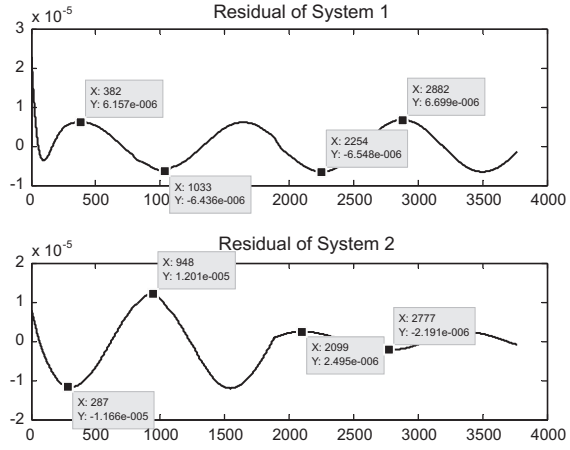

Fig. 7. Residual signals generated for device 1 and device 2. A lower residual signal from samples 0 to 1886 was obtained from device 1 and from samples 1886 to the end from device 2. The maximum and minimum of each residual section is shown in the figure.

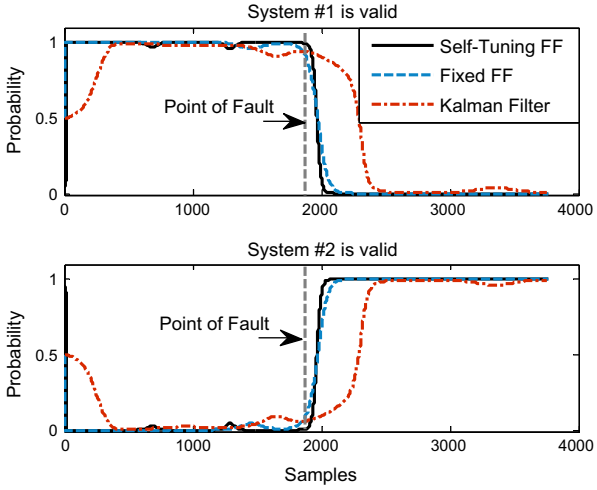

Fig. 8. Fault diagnosis probability densities for device 1 and device 2. Transition performance is provided for the Kalman filter, fixed forgetting factor, and self-tuning forgetting factor techniques.

corresponding residual signal generates a zero average and the lowest in-phase variance. This is shown from samples 0 to 1886 where the fault occurs. The residual signals of two systems (models) show variance values of 1.72e−11 (m) and 6.11e−11 (m) for system 1 and system 2, respectively. As the variance of system 1 is lower, the probability generation and evaluation center should assign higher probabilities to system 1.

In data samples 1886 to the end residual, the variance of system 1 remains higher, as 2.2e−11 (m), but system 2 exhibits a lower variance, 2.5e−12 (m). It should be noted that the variance is generated considering a set of recoded data. Instantaneous comparison of two model outputs with that of the system is not an effective system designation. Zero crossings and considering a threshold level for the fault will eliminate valuable information from the diagnosis. This is more effective if the actual system does not completely match with any of the models. In this case, a linear combination of weighted systems would determine the fault representing model. Hence, the probability density functions and the probability evaluation center are required in this fault diagnosis.

6. Discussion

The self-tuning forgetting factor Eqs. (12)–(18) used in the fault diagnosis of MEMS LCRs were required to be initialized. The initial forgetting factor value and variance as illustrated earlier were considered as $\lambda_0 = 1, \widehat{R}_0 = 0$, with a step size of $\mu = 0.0001$. The fault diagnosis performance can be evaluated in several measures:

6.1. Starting transition

Compared to the parameter in the estimation-based techniques, the Kalman filters reacted to the fault with a delay. The probability transients in the Kalman filter also showed a significant delay compared to the fixed gain estimation technique. The self-tuning gain provided faster transients in the probability evaluation at the point of fault and required fewer overall data samples to diagnose the faults.

6.2. Fault occurrence

The application of Kalman filters, as shown in Fig. 8, resulted in a delay in the diagnosis of the fault in MEMS. The reaction time in both the fixed and the self-tuning forgetting factor was shorter. The transition time was also shorter in the self-tuning forgetting factor when the second fault was introduced at the 1886th data point sample. The Kalman filter's reaction was slow for this application, running at 4000 rad/s.

6.3. During fault

The Kalman filter exhibited smooth probabilities through the diagnosis process. At the point of fault, the Kalman filter showed a delay in the diagnosis of the fault occurrence. The self-tuning forgetting factor resulted in a rapid transition and a stable diagnosis profile. A significant improvement over the Kalman filter and the fixed forgetting factor was achieved by using the self-tuning forgetting factor technique.

7. Conclusion

This paper utilized the self-tuning forgetting factor estimation in fault diagnosis of MEMS LCRs. The performance of fault diagnosis improved significantly in both the transitions and the diagnosis compared to Kalman filters and fixed forgetting factors. Fewer data points were required to diagnose the fault. The variance of the residual signal generated from the closest model to the fault condition was the lowest. This generated higher probability values assigned to the designated model. As the residual signals cross zero and demonstrate a lag in different systems compared to the actual fault-representing system, the diagnosis cannot be accomplished by evaluating the residual signals with respect to a threshold. It was proven that the adaptive forgetting factor could be mapped to positive values of less than one.

References

[1] Rosing R, Richardson A, Dorey A, Peyton A. Fault simulation for MEMS. In: Intelligent and self-validating sensors (Ref. No. 1999/160), Colloquium on IEE. 21 June 1999. p. 7/1–7/6.
[2] Wang L, Dawson JM, Hornak LA, Famouri P, Ghaffarian R. Real time transitional control of a MEMS comb resonator. IEEE Trans Aerosp Electron 2004;40(2).
[3] Park S, Horowitz R, Tan Chin-Woo. Adaptive controller design of MEMS gyroscope. In: IEEE intelligent transportation system conference proceeding, Oakland (CA), USA, August 25–29; 2001.
[4] Izadian. Automatic control and fault diagnosis of MEMS lateral comb resonators, PhD. dissertation, West Virginia University, Lane Department of Computer Science and Electrical Engineering; May 2008.

Please cite this article in press as: Izadian A. Self-tuning fault diagnosis of MEMS. Mechatronics (2013), http://dx.doi.org/10.1016/j.mechatronics.2013.08.006

[5] Fedder GK, Howe RT. Multimode digital control of suspended polysilicon microstructure. IEEE, J Microelectromech Syst 1996;5(4):283–97.
[6] Tang WT, Lim MG, Howe RT. Electrostatic comb drive levitation and control method. IEEE, J Microelectromech Syst 1992;1(4):170–8.
[7] Izadian A. Indirect adaptive trajectory control of MEMS LCR, invited paper. In: Proceeding of IEEE industrial electronic conference, IECON, November 2011.
[8] Bhansali S, Zhang AL, Zmood RB, Jones PE, Sood DK. Prototype Feedback-controlled bi-directional actuation system for MEMS applications. J Microelectromech Syst 2000;9(2):245–51.
[9] Li Y, Horowitz R. Active suspension vibration control with dual stage actuators in hard disk drives. In: Proceedings of American control conference, Arlington, VA, June 25–27; 2001. p. 2786–91.
[10] Pannu S, Chang C, Muller RS, Pisano AP. Closed-loop feedback control systems for improved tracking in magnetically actuated micro mirrors. In: 2000 IEEE/LEOS international conference on optical MEMS; August 21–24, 2000, Kauai, HI,USA. p. 107–8.
[11] Izadian A, Khayyer P, Famouri P. Fault diagnosis of time-varying parameter systems with application in MEMS LCRs. IEEE Trans Ind Electron Invited Paper 2009;56(4):973–8.
[12] Izadian A, Famouri P. Intelligent fault diagnosis of MEMS micro comb resonators using multiple-model adaptive control technique. IEEE Trans Control Syst Technol 2010;18(5):1233–40.
[13] Izadian A, Famouri P. Reliability enhancement of micro comb resonators under fault conditions. IEEE Trans Control Syst Technol 2008;16(4):726–34.
[14] Izadian A, Hornak L, Famouri P. Structure rotation and pull-in voltage control of MEMS lateral comb resonators under fault conditions. IEEE Trans Control Syst Technol 2009;17(1):51–9.
[15] Frank P, Ding S, Koppen-Seliger B. Current developments in the theory of FDI. In: Proceedings of SAFEPROCESS'2000, IFAC, Budapest; 2000.
[16] Hanlon PD, Maybeck PS. Multiple-model adaptive estimation using a residual correlation kalman filter bank. IEEE Trans Aerospace Electron Syst 2000;36(2).
[17] Wang L. Modeling and real-time feedback control of MEMS devices, PhD. dissertation, West Virginia University, Lane Department of Computer Science and Electrical Engineering; May 2004.
[18] Wellstead PE, Zarrop MB. Self-tuning systems control and signal processing. John Wiley & Sons; 1991.
[19] Sorenson HW. Least-squares estimation: from Gauss to Kalman. IEEE Spectr 1970;7:63–8.
[20] Patton RJ, Clark R, Frank PM. Fault diagnosis in dynamic systems: theory and applications. Englewood Cliffs (NJ): Prentice-Hall; 1989.
[21] Zhuang. RLS Algorithm with variable forgetting factor for decision feedback equalizer over time-variant fading channels; 1999.
[22] Hanlon P, Maybeck PS. Multiple-model adaptive estimation using a residual correlation Kalman filter bank. IEEE, Trans Aerospace Electron Syst 2000;36(2):393–406.
[23] Frank PM. Analytical and qualitative model-based fault diagnosis—a survey and some new results. Eur J Control 1996;2:6–28.
[24] Campbell SL, Nikoukhah R. Auxiliary signal design for failure detection. Princeton University Press; 2006.
[25] Isermann R. Supervision, fault-detection and fault-diagnosis methods – an introduction. Control Eng Practice 1997;5(5):639–52.
[26] Rodrigues M, Theilliol D, Adam-Medina M, Sauter D. A fault detection and isolation scheme for industrial systems based on multiple operating models. Control Eng Practice 2008;16:225–39.
[27] Xiong K, Liang T, Yongjun L. Multiple model Kalman filter for attitude determination of precision pointing spacecraft. Acta Astronaut 2011;68(7-8):843–52.
[28] Yu-Ying Guo, Bin JIANG. Multiple model-based adaptive reconfiguration control for actuator fault. Acta Automatica Sinica 2009;35(11).

Please cite this article in press as: Izadian A. Self-tuning fault diagnosis of MEMS. Mechatronics (2013), http://dx.doi.org/10.1016/j.mechatronics.2013.08.006